Molecular Biology of the Cell
Vol. 14, 1058–1073, 2003

Myo3A, One of Two Class III Myosin Genes Expressed in Vertebrate Retina, Is Localized to the Calycal Processes of Rod and Cone Photoreceptors and Is Expressed in the Sacculus

Andréa C. Dosé,*‖ David W. Hillman,† Cynthia Wong,‡ Lorraine Sohlberg,§ Jennifer Lin-Jones,* Beth Burnside*

*University of California, Berkeley, California 94720-3200; †Bayer Pharmaceutical Division, Berkeley, California 94701-1986; ‡University of the Pacific School of Pharmacy, Stockton, California 95211; and §Ingenuity Inc., Mountain View, California 94043

Submitted June 3, 2002; Revised October 2, 2002; Accepted November 6, 2002
Monitoring Editor: Thomas D. Pollard

The striped bass has two retina-expressed class III myosin genes, each composed of a kinase, motor, and tail domain. We report the cloning, sequence analysis, and expression patterns of the long (Myo3A) and short (Myo3B) class III myosins, as well as cellular localization and biochemical characterization of the long isoform, Myo3A. Myo3A (209 kDa) is expressed in the retina, brain, testis, and sacculus, and Myo3B (155 kDa) is expressed in the retina, intestine, and testis. The tails of these two isoforms contain two highly conserved domains, 3THDI and 3THDII. Whereas Myo3B has three IQ motifs, Myo3A has nine IQ motifs, four in its neck and five in its tail domain. Myo3A localizes to actin filament bundles of photoreceptors and is concentrated in the calycal processes. An anti-Myo3A antibody decorates the actin cytoskeleton of rod inner/outer segments, and this labeling is reduced by the presence of ATP. The ATP-sensitive actin association is a feature characteristic of myosin motors. The numerous IQ motifs may play a structural or signaling role in the Myo3A, and its localization to calycal processes indicates that this myosin mediates a local function at this site in vertebrate photoreceptors.

INTRODUCTION

The asymmetrical shapes of the rods and cones of the vertebrate retina are specialized to mediate photon detection and signal transmission. At the distal ends are the outer segments, which are composed of stacks of photopigment-bearing membranous disks surrounded by the plasma membrane. Progressively proximal to the outer segment are the mitochondrion-packed ellipsoid, the endoplasmic reticulum- and Golgi-rich myoid, the perinuclear region, the axon, and the synapse. The outer segment is connected to the rest of the cell by the narrow connecting cilium, through which metabolic fuels and newly synthesized proteins are transported. Although they maintain highly specialized shapes, photoreceptors are not static. Elaborately choreographed morphogenetic movements establish the specialized shapes of photoreceptors during development. Once formed, photoreceptors undergo outer segment turnover throughout life. This turnover is mediated by the daily addition of new disks to the base of the outer segment and the shedding of effete disks from the tip (Young, 1976). Disk addition requires transport of newly synthesized materials from the perinuclear and myoid regions to and through the connecting cilium. More dramatic photoreceptor motility occurs during retinomotor movements of lower vertebrates; light onset induces cone myoids to contract and rod myoids to elongate, whereas dark onset induces opposite movements (Burnside, 1978).

Several observations suggest that the actin cytoskeleton plays an important role in photoreceptor motile processes. Photoreceptors are richly endowed with actin filaments deployed in distinct populations and likely to reflect specialized functional roles. Filamentous actin is concentrated in the distal connecting cilium of the outer segment (Chaitin *et al.*, 1984; Wolfrum and Schmitt, 2000) and throughout the length of the ellipsoid, where it is laterally associated into longitudinal bundles that extend into microvillus-like calycal processes (CPs) that cup the base of the outer segment (Nagle *et al.*, 1986; Arikawa and Williams, 1991). Disruption

Article published online ahead of print. Mol. Biol. Cell 10.1091/mbc.E02–06–0317. Article and publication date are at www.molbiolcell.org/cgi/doi/10.1091/mbc.E02–06–0317.

‖Corresponding author. E-mail address: acdose@socrates.berkeley.edu.

of actin filaments in *Xenopus* photoreceptors by cytochalasin led to the production of oversized outer-segment disks several times the normal diameter, suggesting that actin filaments are required for disk initiation but not for addition of new membrane to disks already initiated (Williams *et al.*, 1988; Vaughan *et al.*, 1989).

Actin-dependent motility may be generated by actin assembly or the interaction of motor proteins with actin filaments. To date, all motor proteins known to translocate along actin filaments are members of the large myosin superfamily (for review, see Berg *et al.*, 2001). They are composed of a conserved globular motor (or head) domain containing the nucleotide- and actin-binding sites, a regulatory neck domain containing binding sites for calmodulin or calmodulin-related light chains (IQ motifs), and a highly variable subclass-specific C-terminal tail domain thought to be responsible for cargo binding and/or targeting of the molecule. The neck domain is considered to act as a lever arm and is thought to be responsible for the primary mechanical component of the power stroke of myosins (Rayment *et al.*, 1993; Houdusse and Cohen, 1996; Highsmith, 1999).

The first myosin to be characterized was the bipolar filament–forming class II myosins of muscle and nonmuscle cells. In contrast to these filament-forming myosins, at least 16 more classes of myosins have been reported from organisms ranging from *Dictyostilium discoidium* to humans (for recent reviews, see Barylko *et al.*, 2000; Hodge and Cope, 2000; Reck-Peterson *et al.*, 2000; Sellers, 2000). None of these "unconventional" myosins appear to form bipolar filaments; thus, they are generally thought to have structural or transport rather than contractile functions.

Class III myosins were the third myosin class discovered and are unique among myosins in having an N-terminal kinase domain attached to the myosin head. The original member of the class III myosins is NINAC of *D. melanogaster*. NINAC is expressed exclusively in fly photoreceptors and has been shown to play roles in photoreceptor maintenance and phototransduction (Porter and Montell, 1993; Porter *et al.*, 1993b; Li *et al.*, 1998). NINAC also associates with the signalplex, a supramolecular signaling complex thought to facilitate the rapid phototransduction cascade in *Drosophila* (Montell, 1998).

A second class III member, MyoIIILim, isolated from the horseshoe crab *Limulus polyphemus,* has also been shown to be expressed exclusively in photoreceptors (Battelle *et al.*, 1998). The first vertebrate class III myosins were recently cloned in our laboratory. We have reported the cloning of two human class III myosins: MYO3A, cloned from the human retina and retinal pigment epithelium (RPE) (Dosé and Burnside, 2000), and MYO3B, cloned from the human retina (Dosé and Burnside, 2000; Berg *et al.*, 2001). It was recently shown that human MYO3A is a target for nonsyndromic progressive hearing loss (Walsh *et al.*, 2002).

Our laboratory has cloned two class III isoforms from retina of the striped bass (*Morone saxatilis*): Myo3A and Myo3B. These were reported previously in meeting abstracts (Hillman *et al.*, 1996; Wong *et al.*, 1998). Here, we present a more detailed characterization of these two bass class III myosins. We provide a sequence analysis of Myo3A and Myo3B, compare them with all class III myosins cloned to date, and examine their tissue expression patterns. We also examine the subcellular localization and the actin- and calmodulin-binding properties of Myo3A.

MATERIALS AND METHODS

Animals

Striped bass, *Morone saxatilis*, were purchased from Chico Game Fish Farm, Chico, CA, and were kept in circular constant-flow indoor tanks containing chloramine-free tapwater at a constant 14:10 light/dark cycle. At 1–2 h before handling, artificial sea salt was added to the tank at a 1:10 dilution, and 15–30 min before handling, bass were treated with 3-aminobenzoic acid ethyl ester (methanesulfonate salt, MS222; Sigma, St. Louis, MO) at 9.4 g/100 gal.

Tissue Dissections

Dark-adapted bass (1 h total darkness) were caught and killed in total darkness and immediately dissected under low light. Light-adapted bass were subjected to bright light (1 h), killed, and dissected in light. Eyes were enucleated, hemisected, and immersed in HBSS (Life Technologies/BRL, Gaithersburg, MD) supplemented with 1 μM calpeptin (Calbiochem-Novobiochem, La Jolla, CA). Similarly, the sacculus was dissected into HBSS/calpeptin. The retina, RPE (dark-adapted) or retina/RPE combined (light-adapted), and sacculus were removed and transferred into either RNA-STAT for preparation of RNA, homogenization buffer, or fresh HBSS/calpeptin for shake-off preparation.

RNA Isolation and cDNA synthesis

RNA was collected from retina and RPE of dark-adapted bass. Total RNA was extracted using RNA-STAT (TEL-TEST, Inc., Friendswood, TX), and m-RNA was purified using the PolyATract mRNA isolation system (Promega, Madison, WI). Rapid amplification of cDNA ends (RACE)–ready cDNA was synthesized from purified mRNA using the Advantage cDNA synthesis kit (Clontech, Palo Alto, CA).

Myo3A and 3B Cloning

A myosin PCR screen was performed on bass retina/RPE cDNA using the degenerate myosin primers ATP-3 and EAF-A (Bement *et al.*, 1994) to amplify the myosins expressed in these tissues. The resultant ~150–base pair PCR products were subcloned, sequenced, and analyzed against GenBank, EMBL, DDBJ, and PDB sequences using the BLAST Network Service of the National Center for Biotechnology Information. Two closely related clones displayed very little sequence similarity to previously identified myosins. The first of these two clones, now called Myo3A, was amplified as four RACE fragments using nested primers designed to amplify in both the 5′ and 3′ directions originating from within the initial 150 base pairs cloned (Hillman *et al.*, 1996).

A 567–base pair fragment spanning the kinase/myosin junction of the second clone, now called Myo3B, was amplified in a separate experiment using two degenerate primers. The upstream primer was directed against a conserved kinase motif GITAIE (GGNATHACNGCNATHGA), and the downstream primer was directed against a conserved motor domain motif NPPHIFAV (CNACNGCRAANAYRTGNGGNGGRTT). It was recognized by sequence comparison as one of the novel clones seen in the original PCR screen described above. Six RACE reactions (one in the 5′ direction and five in the 3′ direction) were performed to clone the cDNA (abstract, Wong *et al.*, 1998).

Northern Blot Analysis

To compare mRNA levels in retina and RPE, 1.7 μg each of RPE polyA RNA and retina polyA RNA were electrophoresed in 1% agarose/formaldehyde gels (Sambrook *et al.*, 1989). Multitissue Northern blots were prepared with 4 μg of polyA RNA from dark-adapted retina, light adapted retina/RPE, brain, heart, intestine, kidney, liver, muscle, and testis. The polyA RNA was transferred to Hybond-N (Amersham Pharmacia Biotech, Piscataway, NJ) by capillary action, and the membrane was prehybridized in 50% formamide, 2× Denhardt's solution, 5× SSC, and 0.1 mg/ml salmon sperm DNA overnight at 42°C and hybridized in the same buffer with the ^{32}P-labeled probes overnight at 42°C. Radioactive labeling of probes was done using Prime-It RmT dCTP labeling reactions (Stratagene, La Jolla, CA), and probes were added at 2 × 10^6 cpm/ml. Membranes were washed in 0.1% SDS/0.1× SSC at 42°C and autoradiographed using x-ray film with intensifying screens at −80°C for up to 1 wk.

Tissue Homogenization and Sample Preparation

Dissected tissue was homogenized in a Teflon/glass motor-driven homogenizer (Eberbach Corp., Ann Arbor, MI) at 180–200 rpm, 40 strokes in one of several buffers: buffer A, 50 mM Mops, pH 7.2, 1 mM EDTA, 1 mM EGTA, 160 mM KCl; buffer B, buffer A + 1 mM dithiothreitol (DTT); buffer C, buffer A + 1 mM DTT and 10 mM ATP; and buffer D, buffer A + 10 mM ATP in the presence of a complex protease inhibitor cocktail (PI): 2 μg/μl aprotinin, 100 μM leupeptin, 1 μM pepstatin, 1 μM calpeptin, 5 μM calpain inhibitor III, 400 μM PMSF, 1 mM benzamidine, 2 mM phenanthroline, 10 μg/μl TAME, 200× protease and phosphatase inhibitor cocktail (P8340, Sigma). The homogenate was subjected to centrifugation (100,000 × *g*); the final supernatant is referred to as high-speed supernatant.

Shake-offs

Shake-offs (isolated photoreceptor inner/outer segments) were prepared by agitating dissected retinas in HBS + calpeptin, breaking off rods and cones at the myoid region. These photoreceptor inner/outer segments are collected by a low-speed centrifugation (1000 × *g*, 20 min, 4°C) and can be either homogenized or further purified on a Percoll step gradient as described (Pagh-Roehl and Burnside, 1995). All gradient purification steps were done in the presence of the protease inhibitor cocktail described above.

Generation of Myosin IIIA Antibodies

Three antibodies were generated against bass Myo3A: a "head" antibody raised against the motor domain (aa 260–669), a "tail" antibody raised against the tail region beyond the last IQ motif (aa 1631–1832), and the "3THDII" (used throughout this study) antibody raised against the extreme C-terminal 22 amino acids. The head and tail domains were expressed as histidine-tagged fusion proteins and injected into rabbits for the production of polyclonal antisera (antibody production was performed at Office of Laboratory Animal Care, University of California, Berkeley). The tail-tip antibody was raised against and affinity-purified on the last 22 amino acids of the bass MYO3A (performed by Bethyl Laboratories, Inc., Montgomery, TX). The epitope chosen for antibody production is at the extreme C terminus (NPYDFRHLLRKTSQRRKLIKQY) in a region almost identical to the human MYO3A tail tip (see Figure 3 for sequence comparison). Currently, an antibody raised against Myo3B suggests that it is not expressed in the photoreceptors.

Western Blotting

Protein samples were subjected to electrophoresis on NuPAGE Tris acetate gels (7%) (Invitrogen, Carlsbad, CA) and transferred to Hybond N (Amersham Pharmacia Biotech) in NuPAGE transfer buffer + 10% methanol and 0.05% SDS. The membrane was blocked with 5% milk in PBS and incubated with 1:80,000 α-3THDII O/N in 3% BSA in PBS at 4°C or 1:5000 immunoaffinity-purified anti-tail antibody. Membrane was washed for 1 h with six changes in PBS and incubated with goat anti-rabbit antibody conjugated to horseradish peroxidase (Amersham Pharmacia) for 1 h at room temperature in 3% BSA in PBS. The membrane was washed again for 1 h with six changes of PBS and developed using enhanced chemiluminescence (Amersham Pharmacia).

Immunocytochemistry

Photoreceptor inner/outer segments were allowed to settle for 5 min on poly-L-lysine–subbed slides and coverslips. They were methanol-fixed in −20°C methanol for 2 min, or paraformaldehyde-fixed in 4% paraformaldehyde/PBS and incubated 40 min at room temperature. After fixation, the slides and coverslips were rinsed twice in PBS. Before immunolocalization, paraformaldehyde-fixed cells were treated with 2% glycine/PBS for 2 min, PBS twice for 2 min, five changes of fresh 0.1 mg/ml sodium borohydride for 5 min, twice with PBS for 2 min, 0.1% Triton-X-100 for 3 min, and twice with PBS for 5 min. Immunolocalization was carried out according to Hoang *et al.* (1999). Secondary antibodies were Alexa 488 (Myo3A) and Cy3 (tubulin) (Molecular Probes, Eugene, Oregon). Phalloidin staining was performed by adding a 1:50 dilution of Texas Red or Alexa 488 phalloidin (Molecular Probes) to the secondary antibody incubation.

Cells were observed with an inverted microscope (Carl Zeiss, Inc., Thornwood, NY) using a 63×/NA 1.4 objective. Images were acquired with a cooled CCD camera (Hamamatsu Corp., Bridgewater, NJ) controlled by Open Lab software (Improvision Inc., Lexington, MA). To obtain images of photoreceptor immunofluorescence and phalloidin staining, section series of 15–25 0.5-μm optical sections were taken. The section series was deconvolved with Open Lab software and merged. Stained photoreceptors were also visualized with a Zeiss 510 Confocal microscope. The Myo3A staining pattern was similar in both methanol- and paraformaldehyde-fixed cells; however, the phalloidin did not label actin filaments in methanol-fixed tissue.

Electron Microscopy

Grids were coated with a thin film of Formvar layered on water. Then, 12–15 coated grids were collected on a coverslip and allowed to air-dry. The grids were then coated with 0.01% poly-L-lysine for 5 min at room temperature and left to dry overnight at room temperature. Freshly prepared ice-cold photoreceptor inner/outer segments were allowed to settle on grids for 5–10 min. Cells were permeabilized for 5–10 min with PHEM buffer (6 mM PIPES, 25 mM HEPES, 8 mM EDTA, 2 mM $MgCl_2$, 1 mM DTT, 20 μM taxol, 25 μg/ml phalloidin) containing 1% Triton X-100. Samples were incubated for 1 hr in blocking buffer: PHEM buffer with 2% BSA and 30% normal goat serum (NGS), followed by a 1-hr incubation in primary antibody diluted (1:200, Myo3A; 1:50, anti-actin) in working buffer (PHEM buffer supplemented with 2% BSA and 10% NGS). The grids were washed three times with working buffer and incubated for 30 min in 1:10 secondary goat anti-rabbit antibody conjugated to 18-mm gold spheres (Jackson Immuno Research, West Grove, PA). Finally, specimens were washed two times in working buffer and once in distilled water, allowed to air-dry, and negative-stained using 1% uranyl acetate.

Rod Inner/Outer Segment Cytoskeleton Extractions

Gradient-purified rod inner/outer segments (RIS/ROS) were collected by centrifugation at 1000 × *g* for 20 min at 4°C and resuspended in buffer B with 1% Triton-X-100 and either 1 mM $MgCl_2$, 1 mM MgATP, or 10 mM MgATP. After 10–20 min on ice, the samples were centrifuged at 100,000 × *g* for 30 min at 4°C. The supernatant

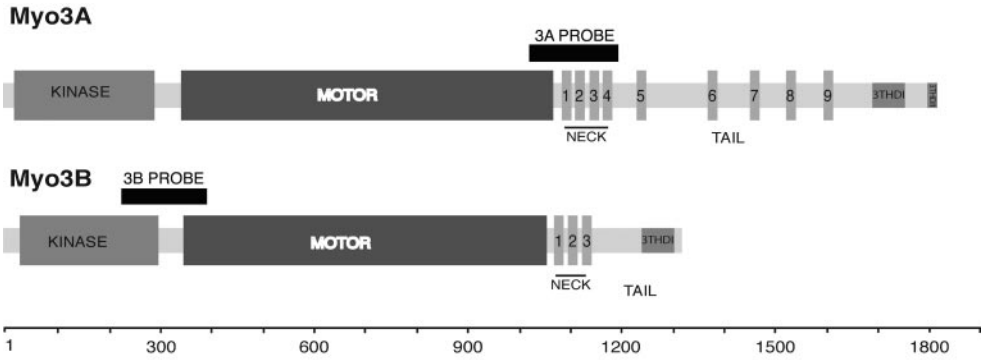

Figure 1. Bar diagrams. This is an alignment of bar diagrams of the two class III myosins cloned in their entirety from *Morone saxatilis* (striped bass): Myo3A (meeting abstract: Hillman *et al.*, 1996), Myo3B (meeting abstract: Wong *et al.*, 1998). Amino acid numbers are depicted below. The kinase and motor core domains are designated. Myo3A and Myo3B contain nine and three putative calmodulin-binding domains consecutively, which are numbered on the bar diagrams. The two conserved class III tail domains are indicated: 3THDI (or PED domain) and 3THDII (or NPYD domain). The lines above the bar diagrams are the regions corresponding to probes for the Northern blots seen in Figure 4.

(cytosolic, peripheral, and membrane proteins) was collected, and the insoluble pellet (cytoskeleton and associated proteins) was resuspended in an equal volume of lithium dodecyl sulfate (LDS) sample buffer (Invitrogen). Samples were electrophoresed and analyzed by Western blotting as described above.

Calmodulin Affinity Column

Cell extract was prepared from homogenized whole retinas as described above. The high-speed supernatant containing the soluble fraction from homogenized retinas was diluted to twice its original volume in HBSS/PI and subjected to centrifugation in a Centricon YM-30 (Millipore Corp., Bedford, MA.) with a 30,000 MW cutoff (as described by Battelle *et al.*, 1998) Once the retinal extract had been reduced to its original volume, it was incubated for 1 h with gentle rocking at 4°C with calmodulin-Sepharose 4B previously washed three times in buffer D/PI (with or without Ca^{2+}). The calcium-containing buffer was generated by adding 2 mM $CaCl_2$ to achieve a calculated free Ca^{2+} concentration of 17 μM (Bers *et al.*, 1994). After the binding step, beads were washed three times in buffer D/PI and incubated with buffer D/PI (with or without Ca^{2+}) for 1–4 h. The bead supernatant was removed, and electrophoresis sample buffer was added directly to the beads to remove any bound Myo3A. The beads were sonicated and pelleted by centrifugation, and the solubilized sample was examined by SDS-PAGE. As a negative control, the same incubations were done with Sepharose beads alone.

RESULTS

Cloning and Characterization of Myo3A and Myo3B

We have previously reported in abstracts that two bass class III myosin isoforms, Myo3A and Myo3B (Figure 1), had been identified during a PCR-based myosin screen performed on the retina and RPE of striped bass (*Morone saxatilis*) (Hillman *et al.*, 1996; Wong *et al.*, 1998). The two myosins were cloned using RACE and identified as class III myosins by virtue of their N-terminal kinase domains. They are a long (Myo3A, 209 kDa) and a short (Myo3B, 155 kDa) isoform with kinase domains that are 66% identical (78% similar), motor domains that are 62% identical (75% similar), and tail domains that are 33% identical (51% similar).

Figure 2 is an unrooted phylogenetic tree of all current myosin classes I–XVIII. All six members of the class III myosins, bass Myo3A and Myo3B, human MYO3A (Dosé and Burnside, 2000) and MYO3B (Dosé and Burnside, 2002), *Drosophila* NINAC (Montell and Rubin, 1988), and *Limulus* $MyoIII_{LIM}$ (Battelle *et al.*, 1998) are compared with one to three representative members of all other myosin classes. The comparison spans the motor domain region corresponding to amino acids 88–780 of chicken muscle myosin (Gg II) (Maita *et al.*, 1991), similar to previously published myosin trees (Cope *et al.*, 1996; Hodge and Cope, 2000).

A clustal W alignment was performed (Figure 3) comparing the predicted amino acid sequence of the bass, human, fruit fly, and horseshoe crab class III myosins used in the tree above. The alignment shows that amino acid sequence similarities lie primarily in the kinase and motor domains and that the tails of these class III myosins are quite divergent. Two isoforms from the same species, bass Myo3A and Myo3B, exhibit a 61% overall identity (75% conserved) to each other in the kinase/motor domain and only 11% identity (16% conserved) in their neck and tail domains.

In the overall alignment of all the class III myosins, the kinase and head domains considered together are 16% identical (31% conserved). The more closely related vertebrate class III myosins are 57% identical (69% similar) in the kinase/motor domains. Insertions occurring in the kinase domains at amino acids 63–69 (in Myo3B) and amino acids 331–346 (in Myo3A) are unique to the bass class III myosins. The two bass class III kinases are 55% identical (66% similar) to MINK, but only in the ~300 amino acids that constitute the kinase catalytic core domain. Near the carboxy-terminal end of the motor domains (945–959 of the consensus sequence), the bass myosin IIIs have insertions of different lengths: 15 amino acids in Myo3A and 8 amino acids in Myo3B relative to the human myosin IIIs. Another insertion at position 1150–1178 of bass Myo3A effectively splits and duplicates an IQ motif, introducing another IQ motif to the neck of Myo3A compared with Myo3B. Both Myo3A and Myo3B have a glutamic acid at the TEDS site (Bement and Mooseker, 1995), suggesting they may be an active motor, unlike NINAC, which breaks the TEDS rule.

Bass Myo3A has nine IQ motifs (putative calmodulin-binding domains) distributed not only within the neck (four), where IQ motifs are found in most myosins, but also throughout the tail (five). Nine IQ motifs is more than have been reported for any other myosin to date. The bass Myo3B has only three IQ motifs; however, this is still more than

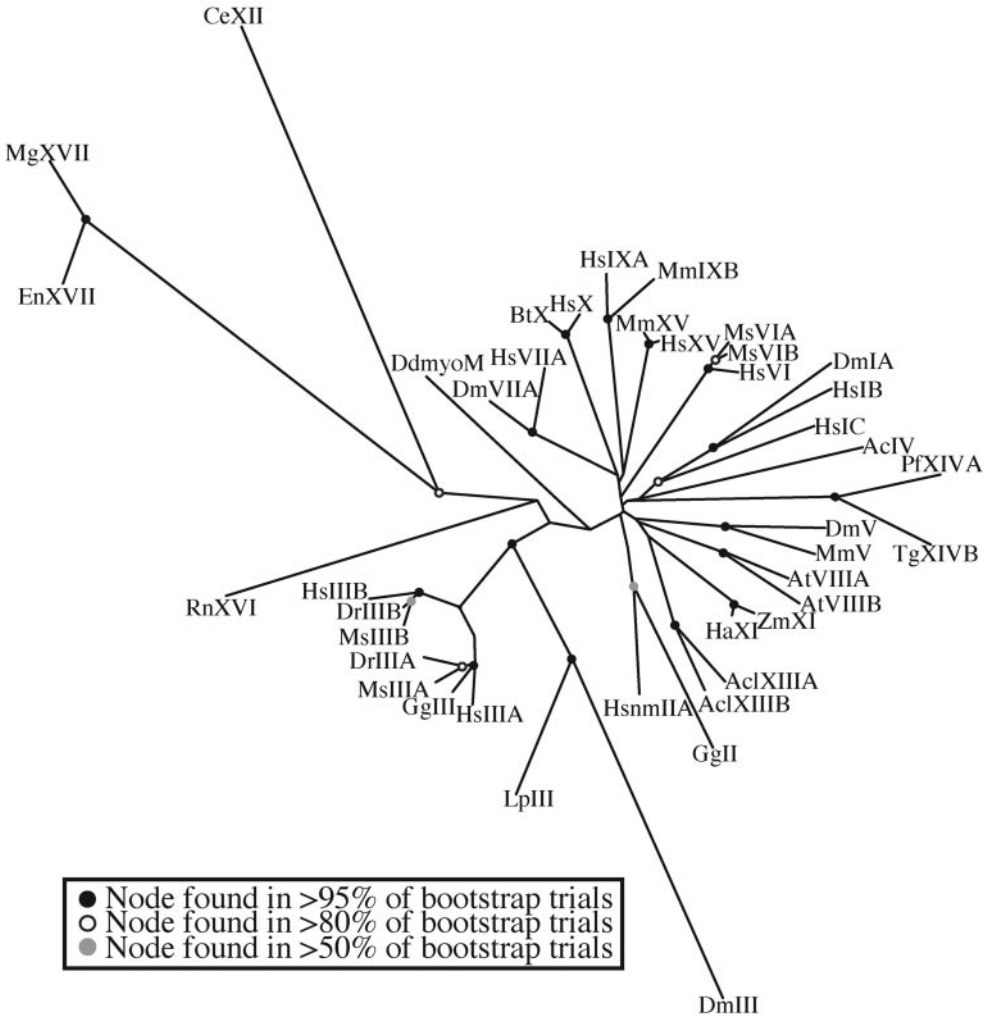

Figure 2. Myosin family tree. An unrooted phylogenetic tree of myosins shows the relationship of class III myosins to the overall myosin family. A clustal-W alignment (http://www2.ebi.ac.uk/clustalw/) was performed on the class III myosins known to date (Montell and Rubin, 1988; Hillman *et al.*, 1996; Battelle *et al.*, 1998; Wong *et al.*, 1998; Dosé *et al.*, 2000; J. Lin-Jones [Gg], L. Sohlberg [Dr], personal communications) and one to three representative myosins from each of 18 classes. Kimura's correction was used and possibly led to the very long branches to DmIII and CeXII. The motor domains corresponding to residues 88–780 of chicken muscle myosin (Gg II) were compared using distance matrix analysis performed with clustal-W (http://bioweb.pasteur.fr/seqanal/interfaces/clustalw-simple.html), and the tree was drawn using TREEVIEW (http://taxonomy. zoology.gla.ac.uk/rod/treeview. html), which was further manipulated in Adobe Illustrator. Ac, *Acanthamoeba casellanii*; Acl, *Acetabularia cliftonii*; At, *Aridopsis thaliana*; Bt, *Bos taurus*; Ce, *Caenorhabditis elegans*; Dd, *Dictyostelium discoidium*; Dm, *Drosophila melanogaster*; Dr, *Danio rerio*; En, *Emiricella nidulans*; Gg, *Gallus gallus*; Ha, *Helianthis annus*; Hs, *Homo sapiens*; Lp, *Liparis polyphemus*; Mg, *Magnaporthe grisea*; Mm, *Mus musculus*; Ms, *Morone saxatilis*; Pf, *Plasmodium falciparum*; Rn, *Rattus norvegicus*; Tg, *Toxoplasma gondii*; Zm, *Zea maize*; nm, nonmuscle. All accession numbers are available on the Myosin Home Page (http://www.mrc-lmb.cam.ac.uk/myosin/trees/accession.html) except Hs MYO3A accession number NM017433, Hs MYO3B accession number NM138995, and Dr Myo3A accession number AF384863.

other shorter class III myosins, such as the short splice variant of NINAC (p132) (Montell and Rubin, 1988), MyoII-ILIM (Battelle *et al.*, 1998), and the human MYO3B (Dosé and Burnside, 2002), which each have one or two IQ motifs. The first four Myo3A IQ motifs and the three Myo3B IQ motifs are evenly spaced, with a periodicity of 26 amino acids between the first amino acids of the IQ motifs, except for the aberrant 28 amino acids between IQ motifs 2 and 3 of Myo3A. Such regularly spaced IQ motifs are a characteristic of the neck domains of all known myosins (Houdusse *et al.*, 1996). Unlike the first four IQ motifs of Myo3A, the next five are scattered throughout the rest of the tail domain. We therefore categorize myosin III IQ motifs as either *neck* or *tail* IQ motifs. The only other known myosin with IQ motifs within its tail domain is the human class III myosin MYO3A (Dosé and Burnside, 2000).

Sequence analysis suggests that the class III myosin tails are not related to other proteins in the database, but the tail and fourth neck IQ motifs are homologous with the previously described GAP-43 module (Neel and Young, 1994). Also, a higher than usual degree of sequence identity (~80%) is shared by the IQ motifs of the tail. The central region in particular is almost perfectly conserved and contains an invariant serine after the glutamine. It is not known whether this site is phosphorylated, but in all five tail IQ motifs, it is within the context predicted to be a serine phosphorylation site by NetPhos 2.0 (http://www.cbs.dtu.dk/services/NetPhos/). It is also interesting that although acidic amino acid residues are rarely found in IQ motifs, an acidic residue occurs in all the tail IQ motifs after the FRGHK sequence.

An extensive search using the coils program (http://www.ch.embnet.org/software/COILS form.html) under stringent conditions identified a 36–amino acid region of Myo3A from 1540–1574 (between IQ motifs 8 and 9) predicted to have a >80% probability of forming a coiled-coil (Lupas, 1996). The predictive scans were made using both the MTK matrix (de-

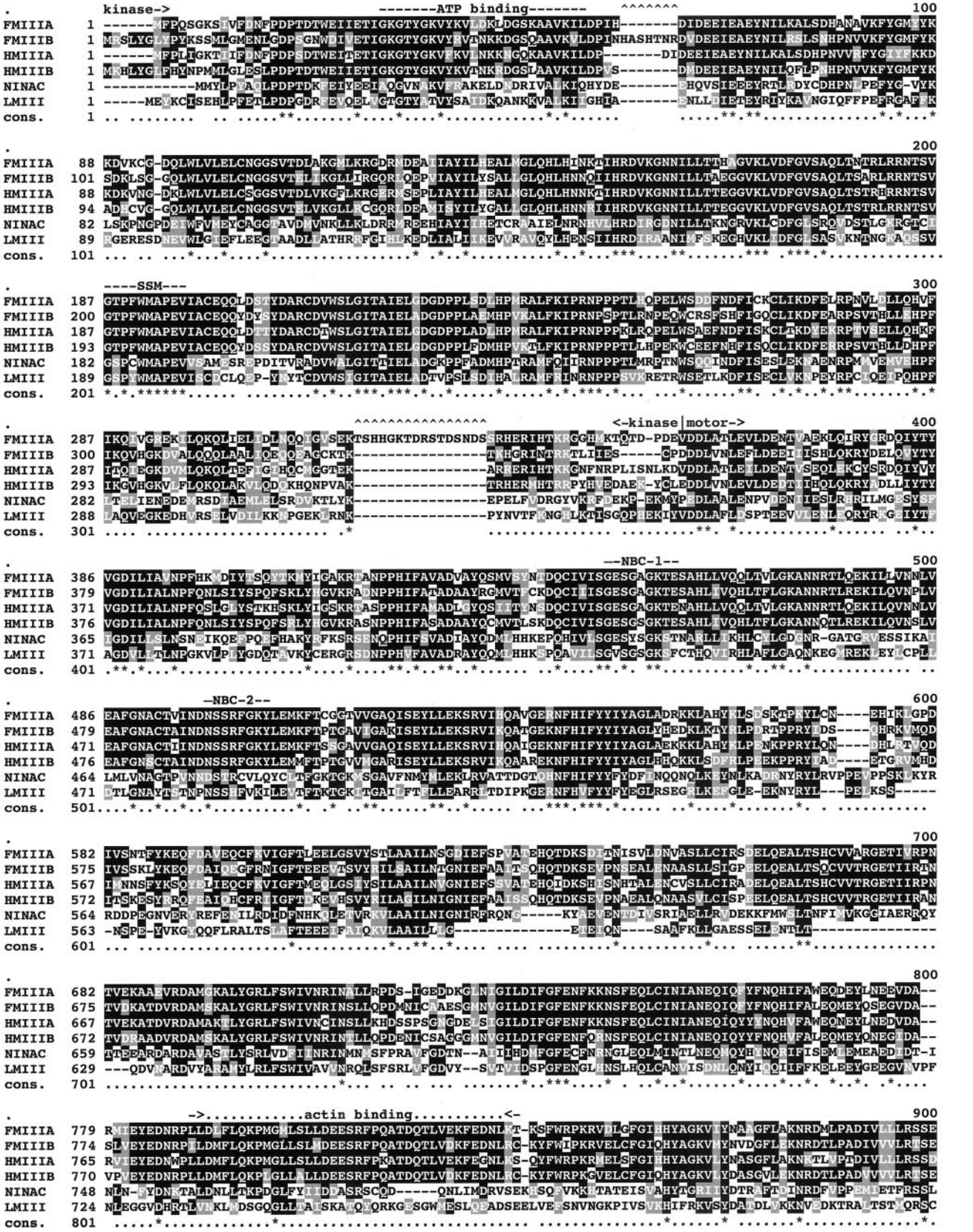
kinase->
-------ATP binding-------
^^^^^^^
<-kinase|motor->
--NBC-1--
-NBC-2--
->.....actin binding.....<-
FMIIIA
FMIIIB
HMIIIA
HMIIIB
NINAC
LMIII
cons.

Figure 3.

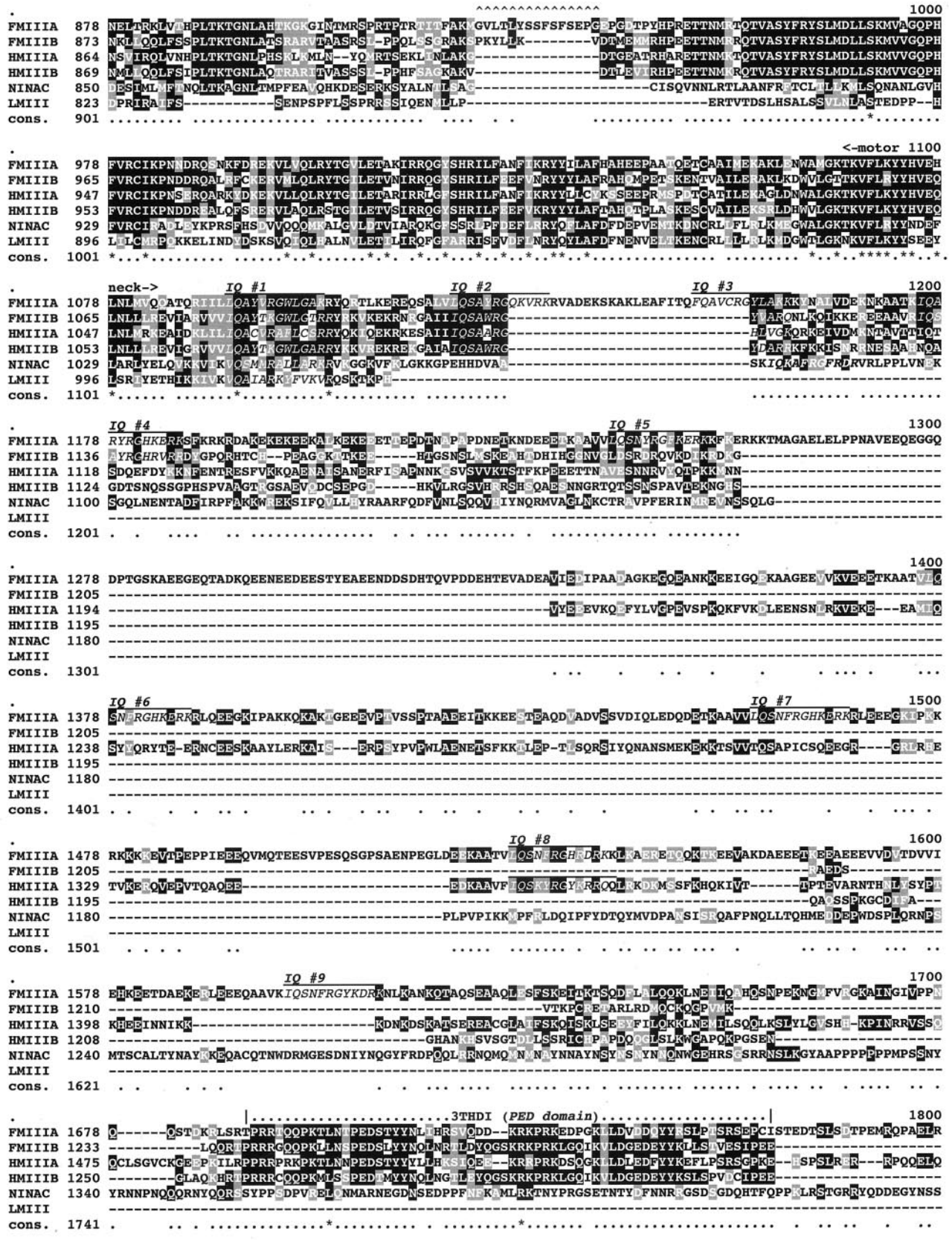
FMIIIA
FMIIIB
HMIIIA
HMIIIB
NINAC
LMIII
cons.
<-motor
neck->
IQ #1
IQ #2
IQ #3
IQ #4
IQ #5
IQ #6
IQ #7
IQ #8
IQ #9
3THDI (PED domain)

Figure 3.

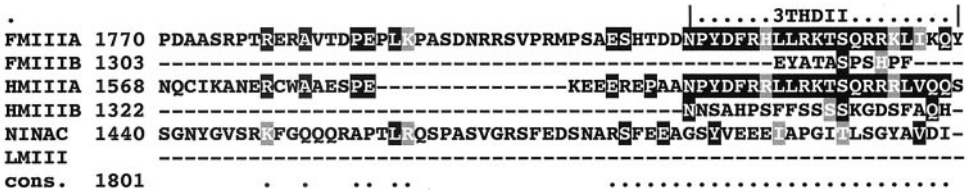

Figure 3 (cont). Amino acid sequence alignment of class III myosins. Boxshade output of a clustal W alignment (Young, 1976) of fish MyoIIIA (designated FMIIIA) and Myo3B (FMIIIB), human MYO3A (HMIIIA), human MYO3B (HMIIIB), *Drosophila* NINAC (DMIII), and *Limulus* $MyoIII_{Lim}$ (LMIII). Black boxes indicate amino acid identity, and gray boxes indicate conserved amino acids. A dot (.) below the alignment indicates conserved amino acids, and an asterisk (*) indicates amino acids that are identical throughout all six class III myosins. The amino acid numbering for the individual sequences are at the left, and the boldfaced numbers above the sequences are for the overall alignment. The junctions between the kinase, head, neck, and tail domains are indicated. Overscored are the ATP-binding site within the kinase (ATP binding); the STE20 family signature motif (SSM); the two conserved ATP-binding regions at the myosin nucleotide binding cleft (NBC-1, or P-loop, and NBC-2); the region implicated in actin binding. The IQ motifs are italicized, and the two vertebrate class III myosin tail homology domains (3THDI and 3THDII) are indicated. Amino acid insertions are indicated (∧∧∧) above the sequence.

rived from the sequences of myosins, tropomyosins, and keratins, intermediate filaments type I and II) and the MTIDK matrix (derived from myosins, paramyosins, tropomyosins, intermediate filaments types I–V, desmosomal proteins, and kinesins). Scans were performed with weighted and unweighted matrices. In all cases, the differences in the probability of forming a coiled-coil were <20%, and the predictions were made using a 28-residue window. The prediction of a coiled-coil domain in the tail of Myo3A remains tentative. Although all criteria for coiled-coil structure are met as specified by the COILS program, the length of 36 residues is only one amino acid above the nominal cutoff for false-positives. Therefore, it remains to be empirically determined whether this region indeed forms a coiled-coil that allows dimerization.

The least conserved regions in the class III myosins are the tail domains; however, among the vertebrate class III tails, there are some striking similarities near their C-termini. There is a 58-amino-acid region that is 43% identical (57% similar) among the vertebrate myosins. We have designated this region the class III tail homology domain I (3THDI). An INTERPRO search (Apweiler *et al.*, 2000) indicates that this region does not resemble any domain or motif currently in the database. At the extreme C-terminus of the bass and the human class IIIA myosins, there is another highly conserved domain that is 77% identical (91% conserved). We have designated this region the class IIIA tail homology domain II (3THDII).

Multiple PEST sequences in Myo3A suggest that this class III myosin may have a short half-life in vivo (Rogers *et al.*, 1986). The PESTfind website at http://www.at.embnet.org/embnet/tools/bio/PESTfind/identified six potential PEST sequences in Myo3A, one at the kinase myosin junction aa 347–372 and five (amino acids 714–723, 1207–1226, 1403–1423, 1482–1521, 1744–1763) near the C terminus (in the tail domain), C-terminal positioning being typical for PEST sequences (Barnes and Gomes, 1995). Such regions contain at least one P, one E or D, and one S or T. They are flanked by lysine (K), arginine (R), or histidine (H) residues, but positively charged residues are disallowed within the PEST sequence. The pest scores range from 8 to 24; the program designates scores of 5 to 50 as strong. Aside from the six strong PEST sequences identified, the program also identified seven weak PEST sequences with scores from −5 to 5. In contrast, the shorter Myo3B contains no strong PEST sequences and only three weak ones. The human IIIA is predicted to have two strong PEST sequences (amino acids 1170–1184 and 1334–1348), which also occur in the tail domain, and three weak sites, and the human IIIB has four weak PEST sequences.

Northern Blot Analysis of Myo3A and 3B

Northern blot analysis was used to examine the expression of Myo3A and 3B in bass retina, RPE, brain, heart, intestine, kidney, liver, muscle, and testis (Figure 4)

Myo3A. Using a motor/tail domain probe (spanning aa 934-1203) (Figure 1), an ~7-kb transcript is labeled in bass retina, brain, and testis (Figure 4). No message was detected in RPE. The level of transcription in the retina is at least 10–50 times higher than that seen in brain and testis.

Myo3B. Using a kinase/myosin junction probe (spanning aa 243–407) (Figure 1), an ~4-kb transcript is labeled in bass

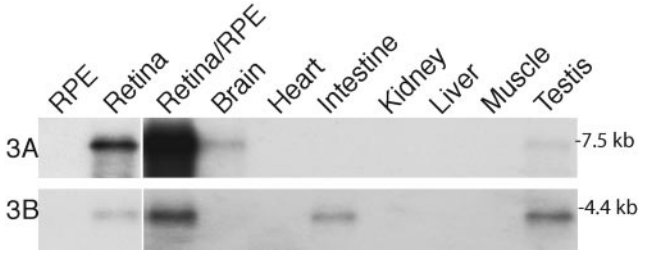

Figure 4. Expression patterns of Myo3A and Myo3B. Two DNA probes were generated for Northern blots: 3A, motor/tail, corresponding to amino acids 934-1203 of bass Myo3A, and 3B, kinase/motor, corresponding to amino acids 243–407 of bass Myo3B; these regions are designated on the bar diagrams in Figure 1. (B) Northern blot: 1.7 μg/lane of dark-adapted retina and RPE mRNA (left) and 4 μg/lane of light-adapted retina/RPE, brain, heart, intestine, kidney, liver, muscle, and testis (right) were probed with Myo3A- and Myo3B-specific probes. Myo3A is expressed at high levels in the retina and at lower levels in the brain and testis. Myo3B is expressed at more similar levels in the retina, intestine, and testis. Despite evidence of Myo3A expression in RPE by Western blot and immunohistochemistry, the Myo3A transcript is below detection levels on our Northern blot.

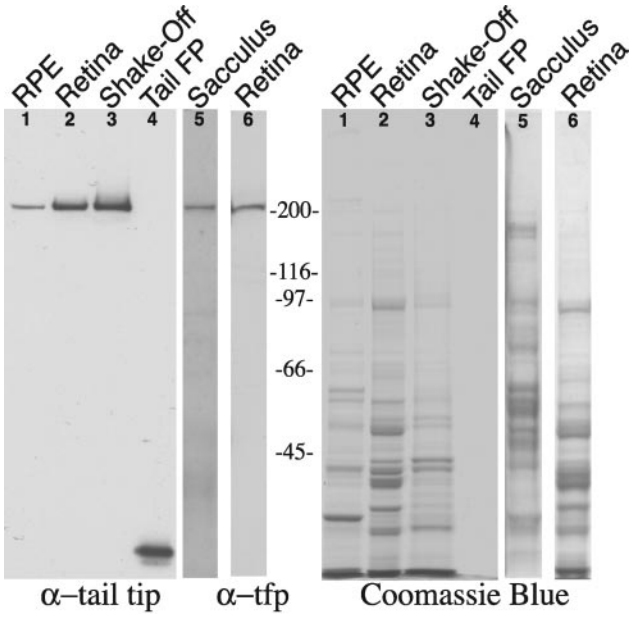

Figure 5. Western blot of Myo3A to determine relative protein levels in the retina and RPE and sacculus. Retina and RPE were dissected separately from dark-adapted bass as well as the sacculus: 9.4 μg of homogenized RPE (lane 1), retina (lane 2), and photoreceptor inner/outer segments (shake-offs) (lane 3) were loaded, and for comparison, 0.02 μg of Myo3A tail fusion protein (lane 4) was included. Also included are ~10 μg of homogenized sacculus (lane 5). An antibody raised against a Myo3A tail-fusion protein also labels the ~200-kDa band (α-tfp, lane 6). The RPE contains significantly less Myo3A than the retina, as does the sacculus (~1/10th as determined by NIH Image), and the Myo3A is enriched in the sample containing photoreceptor inner/outer segments (shake-offs, greater than twofold increase in amount of Myo3A).

retina, intestine, and testis (Figure 4). The transcription levels of Myo3B among tissues tested differ from those seen for 3A in that the 3B levels in retina are similar to the levels in testis and approximately twice that seen in intestine.

Western Blot Analysis of Myo3A

Western blot analysis shows that antibodies to Myo3A label a single band in homogenates of retina, RPE, detached photoreceptor inner-outer segments, and the sacculus of the inner ear (Figure 5). An antibody raised against the highly conserved extreme C-terminal 22 amino acids of Myo3A (which exhibits 77% identity to the human MYO3A) was used to label immunoblotted protein samples from the dark-adapted bass eyes. When isolated, dark-adapted bass retinas are agitated in HBSS, both rods and cones break off at the constricted myoid region, thus generating a suspension of photoreceptor inner/outer segments. The antibody labels a single band at ~210 kDa in the RPE, the retina, the suspension of photoreceptor inner/outer segments, and the sacculus (Figure 5, left). The size of the immunolabeled band is in consistent agreement with the predicted molecular weight of 209 kDa for bass Myo3A. The results show that the level of Myo3A is ~10-fold higher in retina (Figure 5, lane 2) than in RPE (Figure 5, lane 1) or the sacculus (Figure 5, lane 5) and

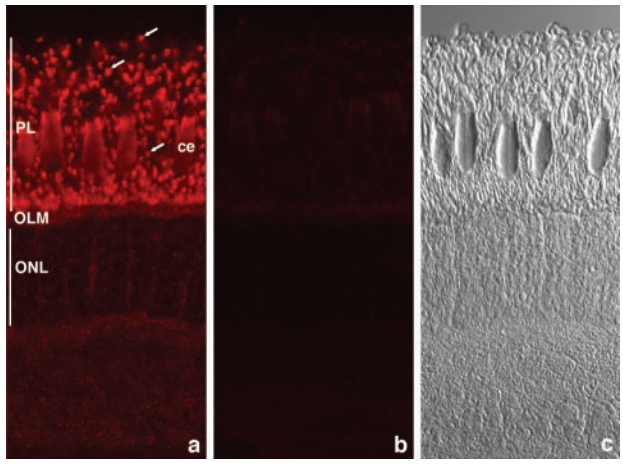

Figure 6. Myo3A immunolabeling of bass retinal tissue sections. Cryosections (8–10 μm) of dark-adapted bass retina were fixed in methanol and immunolabeled. Shown here are the Myo3A labeling (a), Myo3A labeling in the presence of 100-fold molar excess tail-tip peptide (b), and the DIC image (c). Label is concentrated in the distal ellipsoids of both rod and cone photoreceptors, and the specificity of the Myo3A antibody is confirmed by the elimination of epitope recognition in the presence of excess peptide. Cone ellipsoids (ce) and rod ellipsoids are designated by arrows. PL, photoreceptor layer; OLM, outer limiting membrane; ONL, outer nuclear layer. Scale bar, 10 μm.

is also enriched at least twofold in a crude shake-off preparation of photoreceptor inner/outer segments (Figure 5, lane 3). In addition, a secondary antibody raised against a his-tagged tail fusion protein expressing amino acids 1612–1832 of Myo3A also labeled a single 210-kDa band (Figure 5, lane 6). A third antibody generated against the entire motor domain also labeled a 210-kDa band but also labeled multiple other bands in the same sample, suggesting cross-reactivity with other myosins.

Immunolocalization of Myo3A in Retinal Sections

The localization of Myo3A in bass retina was determined from 8- to 10-μm cryosections of dark-adapted bass retina fixed in methanol and immunolabeled with the Myo3A tail-tip antibody (Figure 6). Myo3A labeling of photoreceptors is concentrated in the distal ends of both rod ellipsoids (Figure 6a, arrows) and cone ellipsoids (ce) (red). The specificity of the Myo3A antibody is confirmed by the elimination of epitope recognition in the presence of excess peptide (Figure 6b).

Colocalization of Myo3A and Actin Filaments in Cone Photoreceptors

Isolated inner-outer segments of photoreceptors were labeled with both phalloidin and the anti-Myo3A THDII antibody to ascertain the location of Myo3A in both rods and cones. Figure 7 shows cone inner/outer segments isolated from dark-adapted bass retinas and double-labeled with the Myo3A antibody (Figure 7a, red) and phalloidin (Figure 7b, green); the superimposed image is shown in Figure 7c. Phalloidin (Figure 7, b and c, green) labels actin filament bundles

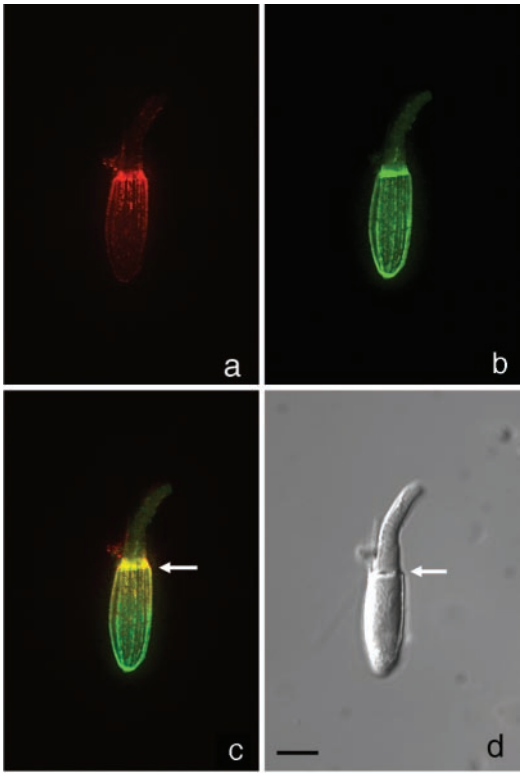

Figure 7. Colocalization of Myo3A and actin in the distal ellipsoid microfilament bundles and CPs of cone photoreceptors. Isolated cone photoreceptor inner/outer segments from dark-adapted bass retinas fixed in 4% paraformaldehyde were double-labeled with anti-Myo3A (a, red) and actin-labeling Alexa 488-phalloidin (b, green). The filamentous nature of the Myo3A staining coincides with the actin filament bundles of the inner segment and CPs at the outer-segment base, and the colocalization is seen as yellow in image overlays (c); (d) DIC image. The white arrows indicate the inner-segment/outer-segment junction. Scale bar, 10 μm.

extending the entire length of the ellipsoid and into the CPs at the inner-segment/outer-segment junction (white arrow). Myo3A labeling (Figure 7a, red; Figure 7c, yellow) colocalizes with the actin bundles in the CPs and the distal end of the ellipsoid but does not colocalize with actin bundles in the proximal ellipsoid. Thus, Myo3A is not generally colocalizing with actin but is specifically localized to bundles in the CPs and the distal ellipsoid.

Localization of Myo3A and Tubulin in Rod Photoreceptors

Myo3A also localizes to the CPs and distal ellipsoid in rod photoreceptors. Figure 8 shows isolated RIS/ROS double-labeled with anti-Myo3A 3THDII antibody (Texas Red secondary) and a monoclonal β-tubulin antibody (Alexa 488 secondary). Tubulin staining (green) is abundant in the myoid and peripheral ellipsoid and in the delicate axoneme of the outer segment. Consistent with the known absence of microtubules from the CPs, the bright tubulin inner segment staining stops short of the inner-segment/outer-segment

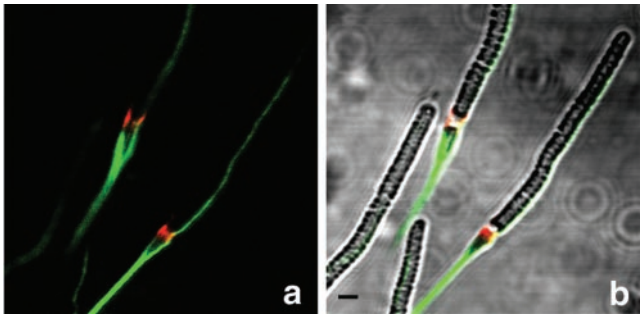

Figure 8. Isolated rod photoreceptors double-labeled with Myo3A and anti-tubulin antibody. RIS/ROS were isolated from dark-adapted green sunfish retinas, fixed in methanol, and double-labeled with the Myo3A antibody (a, red), and anti-tubulin (a, green). An overlay with the DIC image (b, red) demonstrates that the Myo3A antibody labels the inner segment distal to the microtubules, suggesting that it is labeling primarily CPs. Scale bar, 2 μm.

junction (Figure 8, a and b). Myo3A antibody labels the inner segment distal to the microtubule staining. Superimposition of the double-labeled image over the DIC image of the RIS/ROS shows that the Myo3A labeling is at the inner-segment/outer-segment junction, indicating that in rods, as in cones, Myo3A is selectively localized in the CPs and the distal ellipsoid.

Myo3A Is Associated with the Cytoskeleton in an ATP-Dependent Manner

The actin-binding domain of the myosin head binds to actin in an ATP-dependent manner. To investigate whether Myo3A associates with the ellipsoid actin bundles by this mechanism, we examined the partitioning behavior of Myo3A with regard to a purified cytoskeletal fraction of RIS/ROS. We prepared RIS/ROS cytoskeletons by purifying the RIS/ROS on discontinuous-density gradients and extracting them with Triton-X-100 to remove all detergent-soluble components (Pagh-Roehl *et al.*, 1995). The Tx-100 insoluble cytoskeleton was collected by centrifugation in the presence and absence of ATP and probed for with the antibody against Myo3A. In the absence of ATP, the Myo3A is associated with the pelleted cytoskeleton (Figure 9, lanes 1 and 2); in the presence of 1 mM MgATP, however, much of the Myo3A is released from the pellet and is seen in the soluble extraction supernatant (Figure 9, lanes 5 and 6). Increasing the MgATP concentration to 10 mM enhances this release effect (Figure 9, lanes 7 and 8). As a control, 1 mM Mg^{2+} was also tested and did not affect the localization of Myo3A with the cytoskeletal fraction (Figure 9, lanes 3 and 4).

We also examined ATP-dependent association of Myo3A with the RIS/ROS actin cytoskeleton using immunoelectron microscopy (Figure 10). Triton X-100 extraction of isolated RIS/ROS in the presence of the cytoskeletal filament–stabilizing agents phalloidin and taxol leaves behind the intact cytoskeletal "cage" of actin filament bundles and cytoplasmic microtubules. These isolated cytoskeletons retain the shape of the inner segment ellipsoid and myoid as well as preserving the ciliary axoneme and basal bodies (Pagh-Roehl *et al.*, 1992).

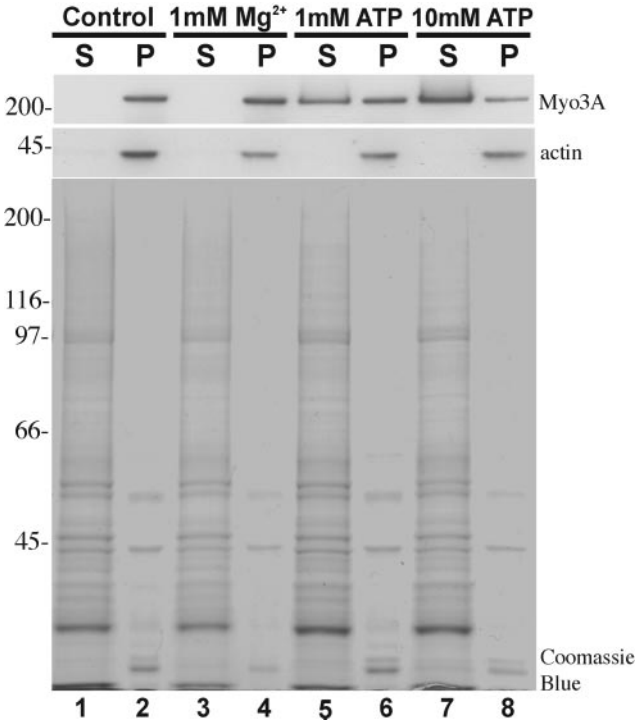

Figure 9. Triton X-100 extractions of RIS/ROS in the presence and absence of ATP. Top (Myo3A): In the absence of ATP (control) and in the presence of Mg^{2+} (1 mM Mg^{2+}), all of the Myo3A associated with the pelleted cytoskeleton (P) and Myo3A was essentially absent from the Triton-solubilized fraction (S). In the presence of 1 mM ATP, some of the Myo3A was released from the cytoskeleton, and in the presence of 10 mM ATP, most of the Myo3A partitions with the supernatant, having been released from the cytoskeleton. Middle (actin): An anti-actin antibody demonstrates that in all cases, actin pellets with the Triton-insoluble fraction (P). Lower (total protein): A Coomassie blue stain shows that the majority of proteins are solubilized in Triton X-100 (S). Only the cytoskeleton and associated proteins are present in the pellet (P).

An anti-Myo3A antibody labels specifically the distal ends of the actin filament bundles; it does not label the actin-rich myoid region or the microtubules of the inner segment or axoneme (Figure 10A). When 10 mM ATP is present during the Triton X-100 extraction, anti-Myo3A labeling of the resultant cytoskeletons is substantially reduced; the number of gold particles associated with the actin filaments is reduced by 85% (eight cytoskeletons examined) (Figure 10B). Gold labeling in the absence of primary antibody is low (Figure 10C). Anti-actin antibodies also specifically label the actin filament bundles in rod cytoskeletons (Dosé, A.C., and Parker, E., data not shown). This control indicated that unlike the Myo3A antibodies, actin antibodies label all parts of the actin cytoskeleton, including the myoid region.

Calmodulin-Binding Properties of Myo3A

Myo3A contains nine IQ motifs. Because the IQ motifs of other myosins have been shown to bind calmodulin in the absence of Ca^{2+}, we sought to characterize the calmodulin-binding properties of Myo3A from retinal extracts in the presence and absence of Ca^{2+}. Retina/RPE extracts were prepared in the presence of ATP and therefore contain soluble Myo3A (Figure 11, left, lane 1). Our results show that Myo3A can bind to calmodulin in the presence and absence of Ca^{2+}. After a 1-hour incubation with calmodulin-Sepharose beads, Myo3A binds to the beads in the absence (Figure 11, left, lane 3) and presence (Figure 11, left, lane 5) of 17 μM free Ca^{2+}. Lanes 2 ($-Ca^{2+}$) and 4 ($+Ca^{2+}$) are the unbound fractions containing Myo3A. More Myo3A is present in the unbound fraction when calcium is present, and these observations are reproducible, suggesting that Myo3A has a higher affinity for calmodulin in the absence of Ca^{2+}. As a negative control, Myo3A was also incubated with Sepharose beads without calmodulin, and the majority of the Myo3a remained in solution (Figure 11, lanes 6 and 7).

DISCUSSION

To examine the role of class III myosins in photoreceptors, we cloned several class III myosins and used sequence comparisons to identify conserved domains that might have functional significance. We also sought functional clues by examining tissue expression patterns, subcellular location, and actin- and calmodulin-binding properties.

Class III Myosins

Class III myosins are widely expressed in vertebrates and invertebrates. Short and long forms are expressed in all species so far examined except *Limulus*. In *Drosophila*, short and long forms are generated by alternative splicing of a single gene, whereas different genes code the two forms of vertebrates. Long and short isoforms of class III myosins have been cloned from bass (meeting abstracts: Hillman *et al.*, 1996; Wong *et al.*, 1998), human (Dosé and Burnside, 2000, 2002; Berg *et al.*, 2001), and zebrafish (L. Sohlberg, unpublished results). A clustal W phylogenetic tree places all known class III myosins on their own branch, but the vertebrate class III myosins are more closely related to each other than either of the invertebrate class III myosins.

The kinase moieties of the class III myosins are members of the germinal center kinase subfamily of the Ste20 group kinases (Sells and Chernoff, 1997; Dan *et al.*, 2000). These kinase/myosin chimeras now constitute their own germinal center kinase subfamily VII (Dan *et al.*, 2000). The kinase domains of Myo3A and 3B most closely resemble Misshapen/NIKs-related kinase (MINK), which has been shown to activate the cJun N-terminal kinase and p38 pathways (Dan *et al.*, 2000). NINAC has been shown to be a functional serine/threonine kinase (Ng *et al.*, 1996).

Among myosins, the motor domain is the most highly conserved region, presumably constrained by the requirements for binding to actin filaments and translocating in an ATP-dependent manner. Motor activity has not been demonstrated for NINAC, with a somewhat divergent P-loop sequence (Montell and Rubin, 1988), giving rise to the question of whether it is a functional motor. The vertebrate class III myosins have more canonical P-loop sequences (seen in the alignment of the NBC-1 in Figure 2), consistent with their being functional motors.

Both vertebrate and *Drosophila* class III myosins bind to F-actin in an ATP-sensitive manner (Hicks and Williams, 1994). Our biochemical and electron microscope studies re-

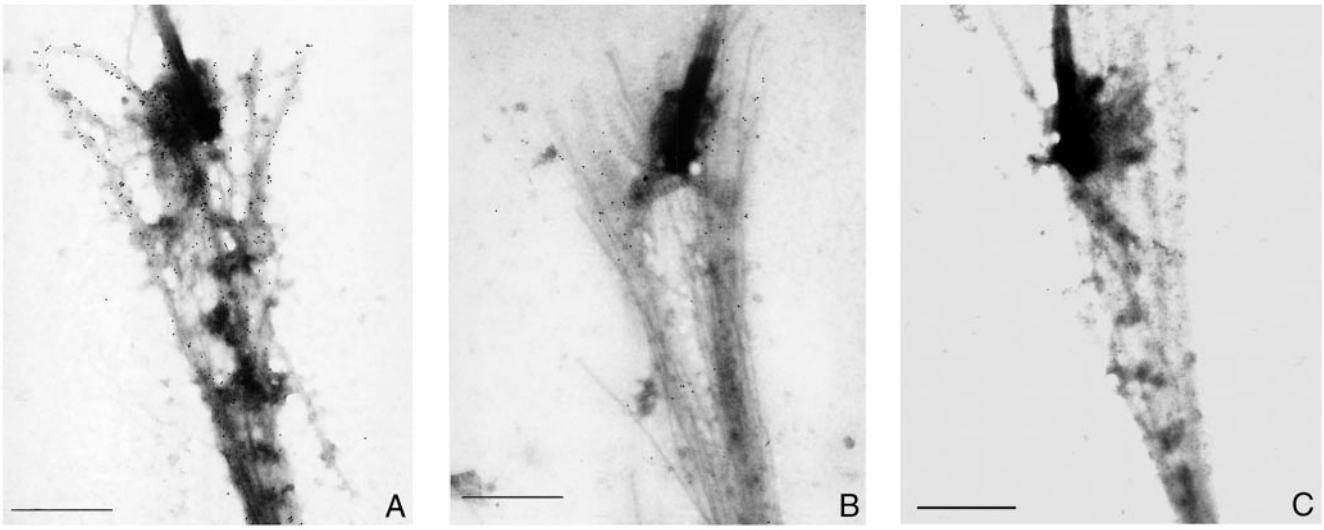

Figure 10. Electron micrographs of rod photoreceptor inner/outer-segment cytoskeletons. The detergent-insoluble fraction of isolated RIS/ROS was isolated and visualized by negative staining. Immunolabeling with an anti-Myo3A antibody abundantly decorates the actin filament bundles, indicating the presence of Myo3A along these filaments (A). The addition of ATP significantly reduces the Myo3A labeling, indicating the release of Myo3A from the actin filament bundles (B). The negative control with no primary shows little labeling (C). Scale bar, 1 μm.

ported here showed that the amount of bass Myo3A associated with isolated photoreceptor inner-segment cytoskeletons was reduced by incubation with ATP. A low affinity for actin in the presence of MgATP has been considered a defining characteristic for myosins, but higher affinities have been associated with processive motors (Mehta *et al.*, 1999).

The neck domain is traditionally defined as the α-helical region that binds essential and regulatory light chains, including calmodulin. Bass Myo3A has four IQ motifs in its neck domain and is unusual in having five additional IQ motifs in its tail domain. The sequence of the last six Myo3A IQ motifs more closely resemble those of GAP-43 (neuromodulin) than the first three myosin neck IQ motifs. GAP-43 (neuromodulin) is a leading candidate for a calmodulin "storage" protein (Toutenhoofd and Strehler, 2000) that may be pertinent to the function of Myo3A.

Like other unconventional myosins, Myo3A binds calmodulin in the absence of calcium. Addition of calcium did not release Myo3A from calmodulin-Sepharose, but the presence of calcium during the incubation reduced the amount of Myo3A bound to calmodulin. Similar studies of myosin I and myosin V have shown that elevated Ca^{2+} results in partial loss of calmodulin binding (Collins *et al.*, 1990; Nascimento *et al.*, 1996); in addition, calmodulin was not dissociated from myosin VI at high Ca^{2+} (Yoshimura *et al.*, 2001). It should be pointed out that binding to calmodulin on a column does not necessarily identify calmodulin as the relevant light chain for Myo3A in vivo. However, in a yeast two-hybrid experiment, the tail of Myo3A used as bait identified only calmodulin as an interactor from a bass retinal cDNA library (Erickson, F.L., unpublished results).

Among the class III myosins, the most divergent regions are the tails; however, two conserved domains were identified in vertebrate class III tails. The 3THDI occurs in all vertebrate class III myosins sequenced thus far, and the 3THDII is a domain seen only in the longer class IIIA myosins. An antibody raised against 3THDII cross-reacts with many species, including chick, rabbit, and rat (Dosé, A.C., unpublished results). The tail of the *Drosophila* class III myosin NINAC interacts with INAD to make it part of the signalplex involved in termination of the phototransduction cascade (Wes *et al.*, 1999).

Expression Patterns and Cellular Localization

Myo3A and Myo3B are expressed in retina, Myo3A at almost 10 times its expression level in brain and testis and Myo3B at twofold to fourfold higher levels than in the testis and intestine. The invertebrate class III myosins NINAC and $MYOIII_{Lim}$ are each expressed specifically in retinal photoreceptors (Montell and Rubin, 1988; Battelle *et al.*, 1998). Retina-enhanced expression was also seen for human MYO3A (Dosé and Burnside, 2000) and MYO3B (Dosé and Burnside, 2002).

The Myo3A transcript was below detectable levels in RPE on Northern blots. Although Myo3A was detected in Western blots of bass RPE, the finding is inconclusive, because dark-adapted RPE is often contaminated with attached photoreceptor inner/outer segments. Preparations enriched for photoreceptor inner/outer segments (shake-offs) were twofold enriched for Myo3A over retina, consistent with the immunohistochemical observation that retinal Myo3A is localized almost exclusively to photoreceptor inner segments. Myo3A was also detected in the bass sacculus on Western blots, confirming in situ hybridization results in fetal mouse cochlea (Walsh *et al.*, 2002). We have also used RT-PCR to amplify MYO3A from a human fetal cochlear library (Dosé, A.C., unpublished results).

Isolated photoreceptor inner/outer segments double-labeled with Myo3A antibody and phalloidin showed Myo3A

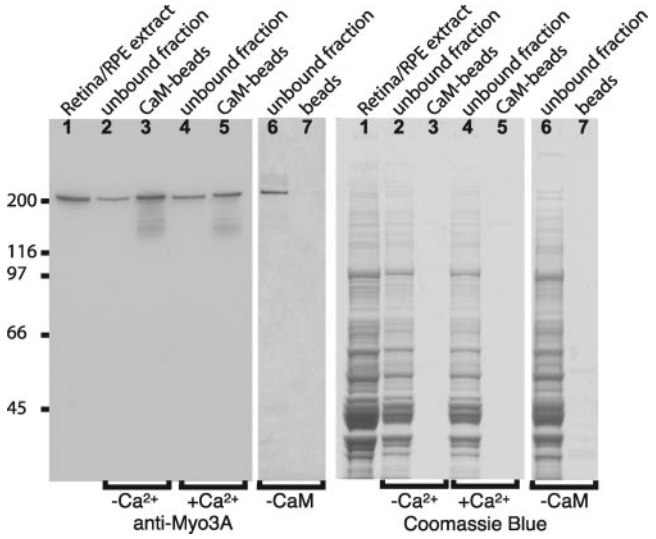

Figure 11. Calmodulin affinity purification of bass Myo3A. The soluble protein fraction of light-adapted retina/RPE homogenate (lane 1) was tested for its ability to bind calmodulin. Like other myosins, bass Myo3A binds to calmodulin in the absence of calcium (lane 3). Having 17 μM calcium present during the incubation of calmodulin-Sepharose beads with retina/RPE extract may reduce the amount of Myo3A that binds to the calmodulin-Sepharose, but in general, the binding seems rather insensitive to calcium (lane 5). Under both conditions, a fraction of Myo3A does not bind calmodulin and remains in solution (lanes 2 and 4). When incubated with Sepharose beads alone, the majority of Myo3A remains in solution (lanes 6 and 7).

colocalizing with the distal portions of ellipsoid actin filament bundles. This polarized localization suggests that the actin interaction is not mediated solely by actin binding. A similar labeling pattern was seen in isolated inner segment cytoskeletons, suggesting relatively robust Myo3A association with the actin bundles. Some but not all of this labeling was lost when cytoskeletons were incubated with ATP, suggesting that binding via the ATP-sensitive actin binding site in the myosin motor domain accounts for some of the binding.

Possible Roles for Myo3A in Photoreceptors

The specific localization of Myo3A to the distal inner segment and CPs suggests that its role may involve CP function. Although CPs were first described almost 40 years ago, their function in vertebrate photoreceptors is still unknown (Brown *et al.*, 1963; Cohen, 1963). Found in almost all vertebrate photoreceptors, CPs are microvillus-like extensions of the inner segment (Borwein, 1981). The core actin filaments of the CPs, with their plus ends distal (Burnside, 1978), originate in the ellipsoid, where they course through the peripheral cytoplasm (Borwein, 1983; Del Priore *et al.*, 1987). The localization of these actin filament bundles suggests that they have a structural role in the inner segment or a role in transport through the inner segment.

It is possible that Myo3A plays a structural role in the CPs, as proposed for brush border myosin-I (Myo1A), which is arranged in spiral tethers that link the microvillar plasma membrane to the actin core filaments (for review, see Mooseker *et al.*, 1991; Coluccio, 1997). There are notable characteristics in common between CPs and the microvilli of intestinal epithelial cells. Both microvilli and CPs contain actin filament bundles with their plus ends distal (Mooseker, 1985; Troutt and Burnside, 1988), and both contain the actin-associated protein fimbrin (Höfer and Drenckhahn, 1993). In the brush border membrane, fimbrin is linked to the lateral plasma membrane by myosin I, which is not present in the CPs (Höfer and Drenckhahn, 1993), and it is possible that myosin III plays a role similar to that of myosin I in cross-linking in photoreceptor CPs.

If myosin III plays a structural role linking the actin bundles to the CP membrane, then some sort of interaction between the III tail and the membrane must exist. Evidence exists for both a microvillar "docking" protein for myosin I and direct interaction of myosin I with phospholipids (for review, see Mooseker *et al.*, 1991). The existence of two highly conserved domains in the tails of class III myosins suggests some sort of binding domain, and studies are under way in our laboratory to identify such interactors. The tail of NINAC binds to the PDZ protein INAD (part of the signalplex), and the tail was sufficient for rhabdomeral localization when fused to β-galactosidase (Wes *et al.*, 1999). The highly conserved regions in the vertebrate tail suggest that they may be critical to their function.

The long NINAC isoform (p174) is expressed in the rhabdomeres, which are functionally analogous to vertebrate outer segments, and the vertebrate myosin III is expressed in the inner segment (CPs). Rhabdomeres, however, are composed of microvilli like the CPs in which Myo3A is localized, and the functions of these two myosins in these similar structures could be the same. The shorter isoform, p132, which localizes to the photoreceptor cell body is not critical, because its deletion did not have an electrophysiological effect or cause retinal degeneration (Porter *et al.*, 1992).

The orientation of the actin filament bundles suggests that Myo3A is a plus-end–directed motor that transports its kinase activity and numerous calmodulins to the CPs. A similar calmodulin transporter role has been suggested for NINAC (Porter *et al.*, 1993a). Myo3A may create a local store of calmodulin that is released in response to changes in calcium concentration or to other signals, such as phosphorylation. A localized calmodulin release would facilitate its diffusion to the outer segment on release, where it has been shown to play an important role in the modulation of the plasma membrane cGMP-gated channel (Hsu and Molday, 1993). It is also possible that Myo3A is not a functional motor but binds and releases actin in an ATP-sensitive manner, or it could localize to the CPs by diffusion, directed there by its tail domain (as seen for myosin I; Tyska and Mooseker, 2002), and once bound, it could exert tension on the CP actin core. Other proteins have been shown to localize to the CPs and may be transported there by Myo3A. Arrestin and the calcium chelation–sensitive ankle-link antigen were localized to the CPs (Mangini and Pepperberg, 1988; Goodyear and Richardson, 1998), and there is brief mention of Na^+,K^+-ATPase localization in CPs (Spencer *et al.*, 1988) and a cGMP binding site (Caretta and Saibil, 1989). The cytoskeletal-associated protein Rab8 has also been shown to localize to CPs (Deretic *et al.*, 1995), and a similar labeling pattern was seen for vitronectin receptor (Anderson *et al.*, 1995). The

actin-filament cross-linking protein fimbrin is associated with the actin filament bundles of CPs and the ellipsoid (Höfer and Drenckhahn, 1993).

Once at the tip of CPs, a plus-end–directed motor would have no obvious exit. Myo3A could possibly move down the CPs passively with retrograde flow of actin bundles, as has been proposed for the translocation of myosin X on the actin filament bundles of filopodia (Berg and Cheney, 2002). Myo3A may ultimately be degraded in the CPs, as suggested by the high number of PEST sequences, a characteristic of proteins with short half-lives of <5 h (Rechsteiner, 1989). This scenario is consistent with the robust mRNA levels of Myo3A but low protein levels in retina. That the protein is easily degraded is further suggested by the extensive protease inhibitor cocktail necessary to purify it intact.

The expression of Myo3A in the inner ear is not surprising, because many other myosins are expressed in these highly specialized actin-rich organs (Hasson *et al.*, 1997; Redowicz, 1999). Mutations in MYO3A cause a nonsyndromic hearing loss without affecting vision (Walsh *et al.*, 2002); however, it is possible that other mutations in the gene may cause both hearing loss and vision defects analogous to the defects seen in patients with different mutations in myosin VII (Petit, 2001).

The specific subcellular localization of Myo3A suggests that it plays some local role in the CPs; however, the function of CPs is not currently understood. The ATP-sensitive association of Myo3A with the photoreceptor actin cytoskeleton and its localization to the plus ends of inner segment actin bundles suggest that it is a functional motor that contributes to its own subcellular localization by walking along the ellipsoid bundles toward the CPs. By this translocation, it simultaneously delivers its own kinase and up to nine calmodulins to the CPs. Other cargoes may also be transported by associating with the Myo3A tail domain. It is not yet clear whether the role of Myo3A is primarily in transport, structural reinforcement, signaling, or some combination of these functions.

ACKNOWLEDGMENTS

The authors thank Ed Parker, Kerri Schwartz, and Angie Zeng, University of California, Berkeley, for technical assistance. This work was supported by National Research Service Award grant EY-06788 to A.C.D. and National Institutes of Health grant EY-03575 and Foundation Fighting Blindness grant to B.B. GenBank accession numbers: for Myo3A, AF003249; for Myo3B, AF512506.

REFERENCES

Anderson, D.H., Johnson, L.V, and Hageman, G.S. (1995). Vitronectin receptor expression and distribution at the photoreceptor-retinal pigment epithelial interface. J Comp Neurol *360*, 1–16.

Apweiler R., *et al*. (2000). Interpro—an integrated documentation resource for protein families, domains, and functional sites. Bioinformatics *16*, 1145–1150.

Arikawa, K., and Williams, D.S. (1991). Alpha-actinin and actin in the outer retina: a double immunoelectron microscopic study. Cell Motil. Cytoskeleton *18*, 15–25.

Barnes, J.A., and Gomes, A.V. (1995). PEST sequences in calmodulin-binding proteins. Mol Cell. Biochem. *149–150*, 17–27.

Barylko, B., Binns, D.D., and Albanesi, J.P. (2000). Regulation of the enzymatic and motor activities of myosin I. Biochim. Biophys. Acta *1496*, 23–35.

Battelle, B.A., Andrews, A.W., Calman, B.G., Sellers, J.R., Greenberg, R.M., and Smith, W.C. (1998). A myosin III from Limulus eyes is a clock-regulated phosphoprotein. J. Neurosci. *18*, 4548–4559.

Bement, W.M., Hasson, T., Wirth, J.A., Cheney, R.E., and Mooseker, M.S. (1994). Identification and overlapping expression of multiple unconventional myosin genes in vertebrate cell types. Proc. Natl. Acad. Sci. USA *91*, 6549–6553; published erratum: (1994) Proc. Natl. Acad. Sci. USA *91*, 11767.

Bement, W.M., and Mooseker, M.S. (1995). TEDS rule: a molecular rationale for a differential regulation of myosins by phosphorylation of the heavy chain head. Cell Motil. Cytoskeleton *31*, 87–92.

Berg, J.S., Powell, B.C., and Cheney, R.E. (2001). A millennial myosin census. Mol. Biol. Cell *12*, 780–794.

Bers, D., Patton, C., and Nuccitelli, R. (1994). A practical guide to the preparation of Ca buffers. Methods Cell Biol. *40*, 3–29.

Borwein, B. (1981). The Retinal Receptor. Berlin, Heidelberg: Springer-Verlag.

Borwein, B. (1983). Scanning electron microscopy of monkey foveal receptors. Anat. Rec. *205*, 363–373.

Brown, P.K., Gibbons, IR., and Wald, G. (1963). The visual cells and visual pigment of the mudpuppy *Necturus.* J. Cell Biol. *19*, 79–106.

Burnside, B. (1978). Thin (actin) and thick (myosinlike) filaments in cone contraction in the teleost retina. J. Cell Biol. *78*, 227–246.

Caretta, A., and Saibil, H. (1989). Visualization of cyclic nucleotide binding sites in the vertebrate retina by fluorescence microscopy. J. Cell Biol. *108*, 1517–1522.

Chaitin, M.H., Schneider, B.G., Hall, M.O., and Papermaster, D.S. (1984). Actin in the photoreceptor connecting cilium: immunocytochemical localization to the site of outer segment disk formation. J. Cell Biol. *99*, 239–247.

Cohen, A.I. (1963). Vertebrate retinal cells and their organization. Biol. Rev. Cambridge Phil. Soc. *38*, 427–459.

Collins, K., Sellers, J.R., and Matsudaira, P. (1990). Calmodulin dissociation regulates brush border myosin I (110-kD-calmodulin) mechanochemical activity in vitro. J. Cell Biol. *110*, 1137–1147.

Coluccio, L.M. (1997). Myosin I. Am. J. Physiol. *273*, C347–C359.

Cope, M.J.T., Whisstock, J., Rayment, I, and Kendrick-Jones, J. (1996). Conservation within the myosin motor domain: implications for structure and function. Structure *4*, 969–987.

Dan, I., Watanabe, N.M., Koboyashi, T., Yamashita-Suzuki, K., Fukagaya, Y., Kajikawa, E., Kimura, W.K., Nakashima, T.M., Matsumoto, K., Ninomiya-Tsuji, J., *et al*. (2000). Molecular cloning of MINK, a novel member of mammalian GCK family kinases, which is up-regulated during postnatal mouse cerebral development. FEBS Lett. *469*, 19–23.

Del Priore, L.V, Lewis, A., Tan, S., Carley, W.W., and Watt, W.W. (1987). Fluorescence light microscopy of F-actin in retinal rods and glial cells. Invest. Ophthalmol. Vis. Sci. *28*, 633–639.

Deretic, D., Huber, L.A., Ransom, N., Mancini, M., Simons, K., and Papermaster, D.S. (1995). Rab8 in retinal photoreceptors may participate in rhodopsin transport and in rod outer segment disk morphogenesis. J. Cell Sci. *108*, 215–224.

Dosé, A.C., and Burnside, B. (2000). Cloning and chromosomal localization of a human class III myosin. Genomics *67*, 333–342.

Dosé, A.C., and Burnside, B. (2002). A new class III myosin expressed in the retina is a candidate for Bardet-Biedl syndrome. Genomics *79*, 621–624.

Goodyear, R., and Richardson, G. (1999). The ankle-link antigen: an epitope sensitive to calcium chelation associated with the hair-cell surface and the calycal processes of photoreceptors. J. Neurosci. *19*, 3761–3772.

Hasson, T., Gillespie, P.G., Garcia, J.A., MacDonald, R.B., Zhao, Y.-D., Yee, A.G., Mooseker, M.S., and Corey, D.P. (1997). Unconventional myosins in inner-ear sensory epithelia. J. Cell Biol. *137*, 1287–1307.

Hicks, J.L., and Williams, D.S. (1994). Myosin III in Drosophila photoreceptors: binding to actin. Invest. Ophthalmol Vis. Sci. *35*, 2130.

Highsmith, S. (1999). Lever arm model of force generation by actin-myosin-ATP. Biochemistry *38*, 9791–9797.

Hillman, D.W., Bost-Usinger, L.M., and Burnside, B. (1996). A potential vertebrate homologue of *Drosophila* NinaC. Mol. Biol. Cell *7*, S:39a.

Hoang, E., Bost-Usinger, L., and Burnside, B. (1999). Characterization of a novel C-kinesin (KIFC3) abundantly expressed in vertebrate retina and RPE. Exp. Eye Res. *69*, 57–68.

Hodge, T., and Cope, M.J.T.V (2000). A myosin family tree. J. Cell Sci. *113*, 3353–3354.

Höfer, D., and Drenckhahn, D. (1993). Molecular heterogeneity of the actin filament cytoskeleton associated with microvilli of photoreceptors, Müller's glial cells and pigment epithelial cells of the retina. Histochemistry. *99*, 29–35.

Houdusse, A., Silver, M., and Cohen, C. (1996). A model of Ca^{2+}-free calmodulin binding to unconventional myosins reveals how calmodulin acts as regulatory switch. Structure (Lond) *4*, 1475–1490.

Hsu, Y-T., and Molday, R.S. (1993). Modulation of the cGMP-gated channel of rod photoreceptor cells by calmodulin. Nature *361*, 76–79.

Li, H.S., Porter, J.A., and Montell, C. (1998). Requirement for the NINAC kinase/myosin for stable termination of the visual cascade. J. Neurosci. *18*, 9601–9606.

Lupas, A. (1996). Prediction and analysis of coiled-coil structures. Methods Enzymol. *266*, 513–525.

Maita, T., Yajima, E., Nagata, S., Miyanishi, T., Nakayama, S., and Matsuda, G. (1991). The primary structure of skeletal muscle myosin heavy chain: IV. Sequence of the rod and the complete 1,938-residue sequence of the heavy chain. J. Biochem. *110*, 75–87.

Mangini, N.J., and Pepperberg, D.R. (1988). Immunolocalization of 48K in rod photoreceptors: light and ATP increase OS labeling. Invest. Ophthalmol. Vis. Sci. *29*, 1221–1234.

Mehta, A.D., Rock, R.S., Rief, M., Spudich, J.A., Mooseker, M.S., and Cheney, R.E. (1999). Myosin-V is a processive actin-based motor. Nature *400*, 590–593.

Montell, C. (1998). TRP trapped in fly signaling web. Curr. Opin. Neurobiol. *8*, 389–397.

Montell, C., and Rubin, G.M. (1988). The Drosophila ninaC locus encodes two photoreceptor cell specific proteins with domains homologous to protein kinases and the myosin heavy chain head. Cell *52*, 757–772.

Mooseker, M.S. (1985). Organization, chemistry, and assembly of the cytoskeletal apparatus of the intestinal brush border. Ann. Rev. Cell Biol. *1*, 209–241.

Mooseker, M.S., Wolenski, J.S., Coleman, T.R., Hayden, S.M., Cheney, R.E., Espreafico, E., Heintzelman, M.B., and Peterson, M.D. (1991). Structural and functional dissection of a membrane-bound mechanoenzyme brush border myosin I. Curr. Top. Membr. *38*, 31–55.

Nagle, B.W., Okamoto, C., Taggart, B., and Burnside, B. (1986). The teleost cone cytoskeleton: localization of actin, microtubules, and intermediate filaments. Invest. Ophthalmol. Vis. Sci. *27*, 689–701.

Nascimento, A.A.C., Cheney, R.E., Tauhata, S.B.F., Larsen, R.E., and Mooseker, M.S. (1996). Enzymatic characterization and functional domain mapping of brain myosin-V. J. Biol. Chem. *271*, 17561–17569.

Neel, VA., and Young, M.W. (1994). Igloo, a GAP-43-related gene expressed in the developing nervous system of Drosophila. Development *120*, 2235–2243.

Ng, K.P., Kambara, T., Matsuura, M., Burke, M., and Ikebe, M. (1996). Identification of myosin III as a protein kinase. Biochemistry *35*, 9392–9399.

Pagh-Roehl, K., Wang, E., and Burnside, B. (1992). Shortening of the calycal process actin cytoskeleton is correlated with myoid elongation in teleost rods. Exp. Eye Res. *55*, 735–746.

Pagh-Roehl, K., and Burnside, B. (1995). Preparation of teleost rod inner and outer segments. Methods Cell Biol. *47*, 83–92.

Petit, C. (2001). Usher syndrome: from genetics to pathogenesis. Annu. Rev. Genomics Hum. Genet. *2*, 271–297.

Porter, J.A., Hicks, J.L., Williams, D.S., and Montell, C. (1992). Differential localizations of and requirements for the two Drosophila ninaC kinase/myosins in photoreceptor cells. J. Cell Biol. *116*, 683–693.

Porter, J.A., and Montell, C. (1993). Distinct roles of the Drosophila *ninaC* kinase and myosin domains revealed by systematic mutagenesis. J. Cell Biol. *122*, 601–612.

Porter, J.A., Yu, M., Doberstein, S.K., Pollard, T.D., and Montell, C. (1993a). The Drosophila NINAC kinase-myosin is a calmodulin-binding protein required for phototransduction and prevention of light-induced retinal degeneration. Mol. Biol. Cell *4*, 153A.

Porter, J.A., Yu, M., Doberstein, S.K., Pollard, T.D., and Montell, C. (1993b). Dependence of calmodulin localization in the retina on the NINAC unconventional myosin. Science *262*, 1038–1042.

Rayment, I., Holden, H.M., Whittaker, M., Yohn, C.B., Lorenz, M., Holmes, K.C., and Milligan, R.A. (1993). Structure of the actin-myosin complex and its implications for muscle contraction. Science *261*, 58–65.

Rechsteiner, M. (1989). PEST regions, proteolysis and cell cycle progression. Rev. Biol. Celular *20*, 235–253.

Reck-Peterson, S.L., Provance, D.W.J., Mooseker, M.S., and Mercer, J.A. (2000). Class V myosins. Biochim. Biophys. Acta *1496*, 36–51.

Redowicz, M.J. (1999). Myosins and deafness. J. Muscle Res. Cell Motil. *20*, 241–248.

Rogers, S., Wells, R., and Rechsteiner, M. (1986). Amino acid sequences common to rapidly degraded proteins: the PEST hypothesis. Science *234*, 364–368.

Sambrook, J., Fritsch, E.F., and Maniatis, T. (1989). Molecular Cloning: A Laboratory Manual, 2nd ed., Cold Spring Harbor, NY: Cold Spring Harbor Laboratory.

Sellers, J.R. (2000). Myosins: a diverse superfamily. Biochim. Biophys. Acta *1496*, 3–22.

Sells, M.A., and Chernoff, J. (1997). Emerging from the PAK: the p21-activated protein kinase family. Trends Cell Biol. *7*, 162–167.

Spencer, M., Detwiler, P.B., and Bunt-Milam, A.H. (1988). Distribution of membrane proteins in mechanically dissociated retinal rods. Invest. Ophthalmol. Vis. Sci. *29*, 1012–1020.

Toutenhoofd, S.L., and Strehler, E.E. (2000). The calmodulin multigene family as a unique case of genetic redundancy: multiple levels

of regulation to provide spatial and temporal control of calmodulin pools? Cell Calcium *28*, 83–96.

Troutt, L.L., and Burnside, B. (1988). Microtubule polarity and distribution in teleost photoreceptors. J. Neurosci. *8*, 2371–2380.

Tyska, M.J., and Mooseker, M.S. (2002). MYO1A (brush border myosin I) dynamics in the brush border of LLC-PK1-CL4 cells. Biophys J. *82*, 1869–1883.

Vaughan, D.K., Fisher, S.K., Bernstein, S.A., Hale, I.L., Linberg, K.A., and Matsumoto, B. (1989). Evidence that microtubules do not mediate opsin vesicle transport in photoreceptors. J. Cell Biol. *109*, 3053–3062.

Vaughan, D.K., and Fisher, S.K. (1989). Cytochalasin D disrupts outer segment disc morphogenesis in situ in rabbit retina. Invest. Ophthalmol. Vis. Sci. *30*, 339–342.

Walsh, T., Walsh, V., Vreugde, S., Hertzano, R., Shahin, H., Haika, S., Kee, M.K., Kanaan, M., King, M.-C., and Avraham, K.B. (2002).From flies' eyes to our ears: mutations in a human class III myosin cause progressive nonsyndromic hearing loss DFNB30. Proc. Natl. Acad. Sci. USA *99*, 7518–7523.

Warrick, H.M., and Spudich, J.A. (1987). Myosin structure and function in cell motility. Annu. Rev. Cell Biol. *3*, 379–421.

Wes, P.D., Xu, X.-Z.S., Li, H.-S., Chien, F., Doberstein, S.K., and Montell, C. (1999). Termination of phototransduction requires binding of the NINAC myosin III and the PDZ protein INAD. Nat. Neurosci. *2*, 447–453.

Williams, D.S., Linberg, K.A., Vaughn, D.K., Fariss, R.N., and Fisher, S.K. (1988). Disruption of microfilament organization and deregulation of disk membrane morphogenesis by cytochalisin D in rod and cone photoreceptors. J. Comp. Neurol. *272*, 161–176.

Wolfrum, U., and Schmitt, A. (2000). Rhodopsin transport in the membrane of the connecting cilium of mammalian photoreceptor cells. Cell Motil. Cytoskeleton *46*, 95–107.

Wong, C.L., Dosé, A.C., and Burnside, B. (1998). A vertebrate homologue of the *Limulus* class III myosin. Mol. Biol. Cell *9*, S:388a.

Yoshimura, M., Homma, K., Saito, J., Inoue, A., Ikebe, R., and Ikebe, M. (2001). Dual regulation of mammalian myosin VI motor function. J. Biol. Chem. (*in press*).

Young, R.W. (1976). Visual cells and the concept of renewal. Invest. Ophthalmol. Vis. Sci. *15*, 700–725.